RSC Advances

PAPER

View Article Online
View Journal | View Issue

CrossMark click for updates

Cite this: *RSC Adv.*, 2014, **4**, 49333

# Acidic ionic liquid supported on silica-coated magnetite nanoparticles as a green catalyst for one-pot diazotization–halogenation of the aromatic amines†

Jalal Isaad*

Received 13th June 2014
Accepted 10th September 2014

DOI: 10.1039/c4ra05705h

www.rsc.org/advances

Acidic ionic liquid was immobilized on silica-coated magnetite nanoparticles ($Fe_3O_4$@SILnP) and used as an efficient heterogeneous catalyst for the diazotization–iodination reaction of different aromatic amines under solvent-free conditions at room temperature. The diazonium salts that are formed by this catalyst are stable at room temperature and react rapidly with sodium iodide to produce aryl iodides in good to excellent yields. This method has some advantages such as low pollution, rapid access to products, simple work-up and easy separation of catalyst from the reaction mixture.

Published on 15 September 2014. Downloaded by Nipissing University on 17/10/2014 17:30:54.

## Introduction

The synthesis of azo compounds is highly important for different uses such as organic dyes,[1–11] chemosensors,[12–17] indicators,[18] radical polymerization initiators,[19] and photochemical switches.[20,21] Azo dyes can be obtained *via* condensation of diazonium salts with a strong nucleophile. Diazonium salts are prepared by the reaction of nitrosonium ion ($NO^+$) and aniline derivatives in low temperature (0–5 °C). $NO^+$ ions are achieved *via* reaction of sodium nitrite and strong liquid acids such as silica sulfuric acid,[22] sulfanilic acid,[23] *p*-toluene sulfonic acid,[24] potassium hydrogen sulfate under solvent free condition,[25] nano sized iron-promoted,[26] zinc and ammonium salts.[27] Also, the azo compounds are prepared by the oxidation of hydrazines,[28–30] reduction of azoxybenzenes,[31–33] and reductive coupling of nitroaromatics.[34–36] However, the most of these techniques have limitations such as long reaction time, toxic materials and tedious work-up.

On the other hand, the use of the ionic liquid as heterogeneous catalysts under solvent-free conditions is becoming very popular as it has many advantages such as reduced pollution, reusability, high selectivity, low cost, and simplicity in process and in handling. These factors are especially important in industry. These advantages led to the use of ionic liquids in the synthesis of azo dyes.[37–39]

In this sense, Brønsted acidic ionic liquids are important class of ionic liquids and form by the transfer of a proton between a Brønsted acid and a Brønsted bases. The key property of these ionic liquids is their Brønsted acidity, and much research has been conducted into this.[40,41] They have been used as catalysts and/or media instead of inorganic acids in many conventional synthetic reactions. Since the most organic compounds can dissolve in ionic liquids, acidic ILs can be used both as reaction medium and solvent.[42] Though ILs possessed such promising advantages, their widespread practical application was still hampered by several disadvantages, for examples (a) high viscosity, which resulted in only a minor part of ILs taking part in the catalyzed reaction for chemical production (b) homogeneous reaction, which was difficult for separation and reuse procedures (c) consequently high cost for the use of relatively large amounts of ILs as opposed to economic criteria.[43,44]

An approach to overcome these limitations is the development of supported ionic liquid catalysts (SILC) that requires smaller amounts of ionic liquid and simultaneously minimizes limitations associated to their viscosity, separation and corrosiveness. SILC combine attractive features of homogeneous catalysis such as the uniform nature of the catalytic centres, high specificity and selectivity of the catalyst, with important features of heterogeneous catalysts, such as high interfacial surface area, high system stability, reusability and potential use in fixed-bed reactor.[45] SILC have been successfully used as catalysts in various organic reactions, for example hydroformylation,[46,47] alkylations,[48] and hydrogenation;[49,50] reaction.

Recently, the functional silica and silica-coated magnetite nanoparticles are considered the most active research areas in advanced materials, they were used as a support for different application such as the dehydration of fructose to 5-hydroxymethylfurfural,[51] and heavy metals chemosensing.[52,53] Additionally, recent studies show that silica coated magnetite nanoparticles are excellent supports for catalysts.[54] The

*Lille Nord de France University, Engineering and Textile Materials Laboratory, Lille, France. E-mail: jalal.isaad@ensait.fr; Tel: +33 3 20 25 86 87*

† Electronic supplementary information (ESI) available. See DOI: 10.1039/c4ra05705h

Published on 15 September 2014. Downloaded by Nipissing University on 17/10/2014 17:30:54.

supported catalysts proved to be effective and easily separated from the reaction media by applying an external magnetic field.

The main objective of the present study is the development of a new class of supported ionic liquid catalysts (SILC). An acid ionic liquid with catalytic activity based on *N*-propyl-2-pyrrolidonium hydrogen sulfate ([H-NMP]$HSO_4$) moiety has been covalently bound to nano-sized silica-coated magnetite to produce supported Ionic liquid nanoparticles ($Fe_3O_4$@SILnP) as reported in the Fig. 1. In particular, these systems have been developed to acquire the advantages of heterogeneous catalytic systems and the large surface area that is conferred by the nanoparticles.

To evaluate the size effects originating from the silica coated magnetite supports, particles with different sizes are evaluated on the catalytic performance in the diazotization reaction. The reusability of the $Fe_3O_4$@SILnP has been also investigated at the optimized reaction conditions reported in this work.

## Results and discussion

### Synthesis of *N*-(propyl-triethoxysilane)-2-pyrrolidone

The Scheme 1 reports the synthesis of *N*-(propyl-triethoxysilane)-2-pyrrolidone **3b** from pyrrolidin-2-one **1** witch reacts with (3-chloropropyl)triethoxysilane **2** in dry toluene under reflux for 24 h followed by the treatment with sulfuric acid.

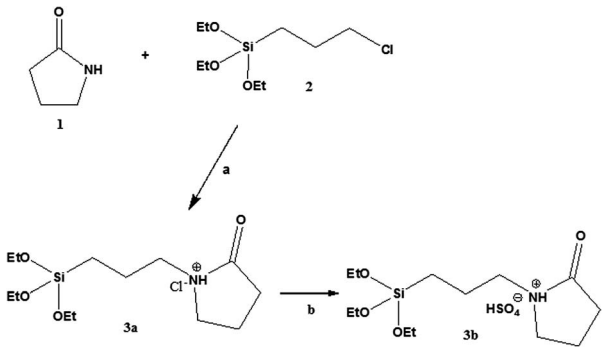


Scheme 1 Synthesis of *N*-(propyl-triethoxysilane)-2-pyrrolidone. Reagents and condition (a) dry toluene, reflux, 24 h (b) $H_2SO_4$, DCM, 0 °C to 60 °C, 12 h.

### Synthesis and surface modification of silica-coated magnetite nanoparticle catalysts

The magnetite nanoparticles were prepared following the procedure reported in the literature.[55] The coating magnetite nanoparticles with silica was carried out by using the sol–gel process, relies on the use of the of tetraethyl orthosilicate (TEOS) as the source of silica matrix. In this method, silica phase are formed on colloidal magnetic nanoparticles in a basic alcohol–water mixture of absolute EtOH, DIW, and 30% aq ammonia solution. After, the surface of the prepared silica

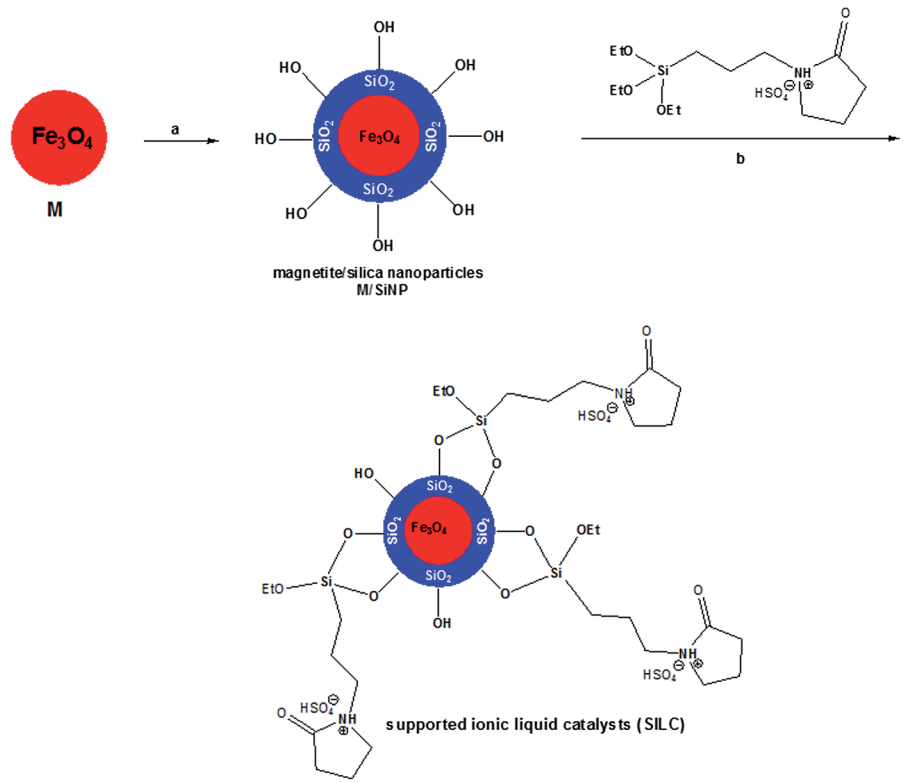


Fig. 1 General structure of the supported ionic liquid catalysts ($Fe_3O_4$@SILnP) based on *N*-propyl-2-pyrrolidonium hydrogen sulfate ([H-NPP]$HSO_4$) bonded to nano-sized silica-coated magnetite. (a) $H_2O$/EtOH/$NH_3$ aq, sonication, TEOS, 12 h (b) toluene, reflux, 24 h.

 This journal is © The Royal Society of Chemistry 2014

Published on 15 September 2014. Downloaded by Nipissing University on 17/10/2014 17:30:54.

nanoparticles was modified by the ionic liquid **3b** containing the organosilane moiety.

### Catalyst characterization

The structural information of the supported ionic liquid nano particles ($Fe_3O_4$@SILnP) was studied by solid-state characterization techniques such as TEM imaging, TGA, VSM and FTIR.

The TEM images of the magnetite, the silica coated magnetite, and the modified silica coated magnetite ($Fe_3O_4$@SILnP) nanoparticles used in this study are shown in Fig. 2.

The silica coated magnetite nanoparticles present a spherical shape with an average particle diameter of about 55 nm. When the silica coated magnetite nanoparticles were functionalized with the ionic liquid based on the *N*-(propyltriethoxysilane)-2-pyrrolidone **3b**, the obtained nanoparticles show a little aggregation comparing with the silica coated magnetite nanoparticles which might be because the layer of ionic liquids surrounding may interact with each other.

The magnetic properties of the synthesized nanoparticles were also studied by a vibrating-sample magnetometer VSM. Fig. 3 shows the hysteresis loops of the $Fe_3O_4$; silica coated $Fe_3O_4$ and supported ionic liquid nano particles ($Fe_3O_4$@SILnP) at room temperature. The saturation magnetization, $M_s$, of bulk magnetite (92 emu $g^{-1}$) was reduced to 57 emu $g^{-1}$ for magnetite nanoparticles. It is known that the magnetization of a magnetic particle in an external field is proportional to its size value. Therefore, a smaller saturation magnetization value for the magnetite nanoparticles compared to the bulk material is reasonable. The saturation magnetic moments of the silica coated $Fe_3O_4$ nanoparticles and the $Fe_3O_4$@SILnP reached to 48 emu $g^{-1}$ and 41 emu $g^{-1}$, respectively. This can be explained by considering the diamagnetic contribution of the silica shells surrounding the magnetite nanoparticles.

The thermal stability of samples was investigated by thermogravimetric analysis (TGA). TGA curves of the magnetite, silica coated magnetite and magnetic silica nanoparticles modified with ionic liquids are shown in Fig. 4. As shown in Fig. 4, the weight losses of the magnetic silica nanoparticles modified with ionic liquids $Fe_3O_4$@SILnP (curve 3) below 250 °C were resulted from the release of both the physisorbed and chemisorbed water on the surface of the $Fe_3O_4$@SILnP nanoparticles. And the breakout of the structured water in SILnP occurred above 600 °C. The organic compounds of $Fe_3O_4$@SILnP were decomposed in the temperature range of 250–600 °C. The major weight loss is attributed to the decomposition of fixed ionic liquid which is chemically bonded onto the surface of magnetite coated silica nanoparticles. The amount of organic compounds bound on the surface of the nanoparticles is estimated from the percentage of weight loss from the TGA curve. TGA of the in $Fe_3O_4$@SILnP indicated that the fixed ionic liquid content was about 12%.

The fixed ionic liquid started to decompose at about 250 °C and was completely burned out at about 595 °C. For the unmodified magnetite coated silica, no significant weight loss below 100 °C could be observed and only a small change in mass percentage could be seen in the temperature range of 100–250 °C. The weight loss recorded as 2 wt% in this temperature range mainly resulted from the release of water molecules bonded physically and chemically in the magnetite nanoparticles (Fig. 4A).

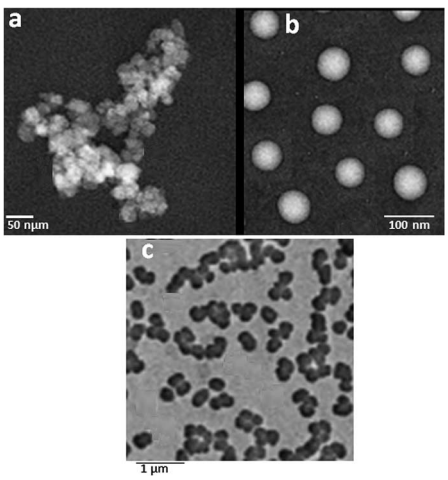


Fig. 2 The micro-pictures of (A) naked $Fe_3O_4$ particles (TEM); (B) magnetic silica nanoparticles (TEM); (C) magnetic silica nanoparticles modified with ionic liquids.

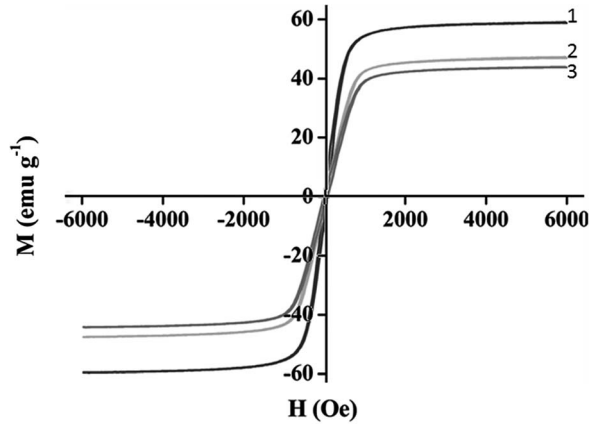


Fig. 3 Magnetization curve of (1) magnetite nanoparticles (2) silica coated $Fe_3O_4$ and (3) magnetic silica nanoparticles modified with ionic liquids.

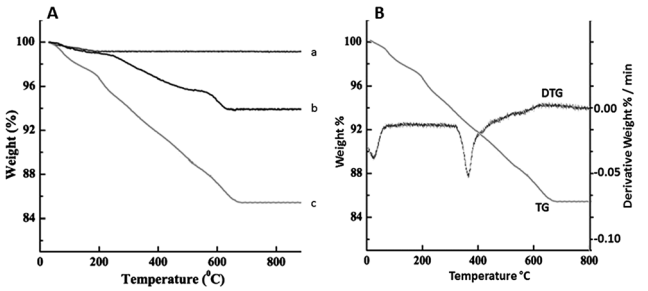


Fig. 4 (A) Thermogravimetric (TG) curves for (a) magnetite (b) silica coated magnetite and (c) magnetic silica nanoparticles modified with ionic liquids (SILnP) and (B) TG-DTG of $Fe_3O_4$@SILnP.

Published on 15 September 2014. Downloaded by Nipissing University on 17/10/2014 17:30:54.

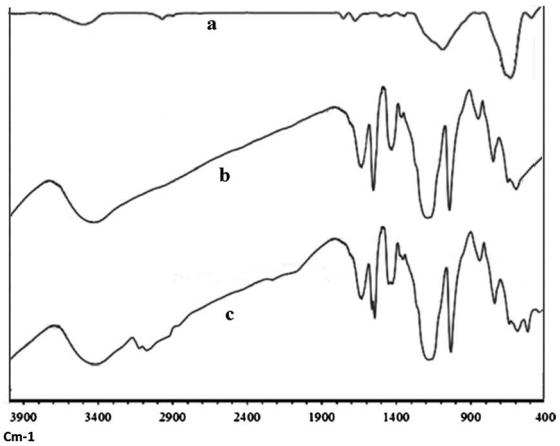


Fig. 5 FT-IR Spectrum (a) silica coated $Fe_3O_4$, (b) [H-NPP]$HSO_4$ ionic liquid and (c) magnetic silica nanoparticles modified with ionic liquids.

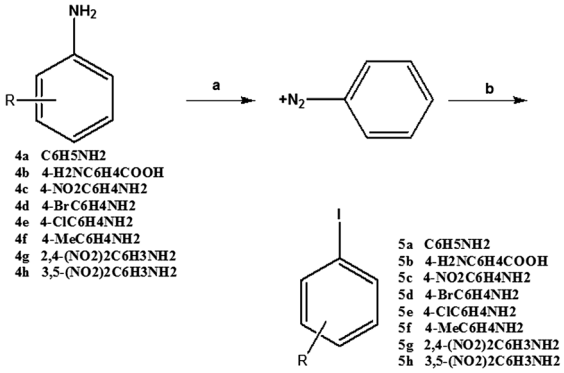


Scheme 2 Synthesis of the aryl iodide **5a–f** by using $Fe_3O_4$@SILnP as catalyst. Reagents and conditions (a) $NaNO_2$, $Fe_3O_4$@SILnP, drops of $H_2O$, 0 °C (b) NaI, 0 °C to RT.

Meanwhile, the peak in the DTG curve (Fig. 4B) shows that the fastest loss of the IL occurred at 390 °C. Therefore, the $Fe_3O_4$@SILnP is stable around or below 250 °C. These TGA analyses indicated that the silica coated $Fe_3O_4$ particles were covered successfully by the coupling with the ionic liquid **3b**.

In the FT-IR spectrum, of the silica coated $Fe_3O_4$ (Fig. 5a) show the stretching vibrations at 590, 950, 1090, 1630 and 3400 $cm^{-1}$ corresponding to the Fe–O, Fe–O–Si, Si–O–Si, and water (free or adsorbed water that still remained in the sample) stretches respectively. However, in the case of the magnetic silica nanoparticles modified with ionic liquids (Fig. 5c), the characteristic peaks of the $Fe_3O_4$@SILnP around 1035 $cm^{-1}$, 1180 $cm^{-1}$ which were attributed to S=O asymmetric and symmetric stretching vibrations of the $-SO_3H$ group, and peaks around 1549 $cm^{-1}$ and 1696 $cm^{-1}$ correspond to the stretching vibrations of the amidic N–H and C=O groups respectively. The bands at 2995 $cm^{-1}$ correspond to the carbon chain ($CH_2$) of the pendant group attached to the inorganic matrix. Therefore, it indicated that the silica coated $Fe_3O_4$ were successfully coated with the ionic liquids.

### Catalytic activity of the catalyst

The catalytic activity of $Fe_3O_4$@SILnP was studied in the diazotization reaction of the aniline derivatives **4a–f** to synthesis its corresponding aryl halide derivatives **5a–f** by the treatment of the formed diazonium salts with NaI as reported in the Scheme 2.

Different aromatic amines possessing electron-withdrawing or electron-donating groups were transformed rapidly into the corresponding aryl iodides in good yields under solvent-free conditions as shown in Table 1. However, the weakly basic aromatic amines 2,4-dinitroaniline and 3,5-dinitroaniline were converted into the corresponding iodoarenes in moderate yields (Table 1, entries 7 and 8). An advantage of this procedure is that the corresponding phenol by-products were formed only in trace yields. The effect of the solvent on this reaction was also studied. The use of water as solvent, under the same conditions,

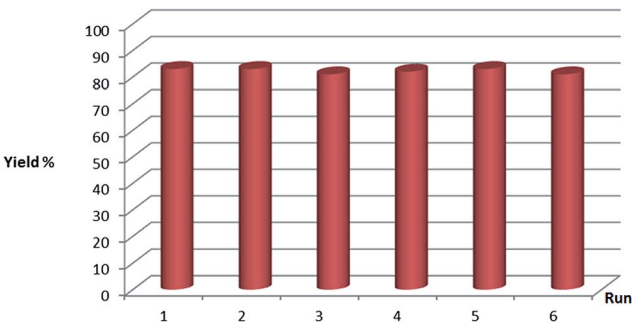


Fig. 6 Reuse of $Fe_3O_4$@SILnP in the diazotization–iodination of 4-$NO_2C_6H_4NH_2$.

Table 1 Iodination of aromatic amines with $Fe_3O_4$@SILnP/$NaNO_2$/NaI/at 0 °C to room temperature

| Entry | Substrate | Time diazotization–iodination | Yield | Mp (°C) | Lit. mp (°C) |
|---|---|---|---|---|---|
| 1 | $C_6H_5NH_2$ | 6/6 | 73 | Oil | Oil[56] |
| 2 | 4-$H_2NC_6H_4COOH$ | 8/6 | 95 | 268–270 | 269–270 (ref. 56) |
| 3 | 4-$NO_2C_6H_4NH_2$ | 10/4 | 83 | 171–172 | 172–173 (ref. 56) |
| 4 | 4-$BrC_6H_4NH_2$ | 8/4 | 78 | 88–89 | 89–91 (ref. 56) |
| 5 | 4-$ClC_6H_4NH_2$ | 8/4 | 82 | 55–56 | 55–56 (ref. 56) |
| 6 | 4-$MeC_6H_4NH_2$ | 9/6 | 62 | 34–35 | 35–37 |
| 7 | 2,4-$(NO_2)_2C_6H_3NH_2$ | 15/10 | 43 | 88–89 | 88.5–89.0 (ref. 56) |
| 8 | 3,5-$(NO_2)_2C_6H_3NH_2$ | 15/10 | 51 | 97–99 | 99–100 (ref. 56) |


This journal is © The Royal Society of Chemistry 2014

Published on 15 September 2014. Downloaded by Nipissing University on 17/10/2014 17:30:54.

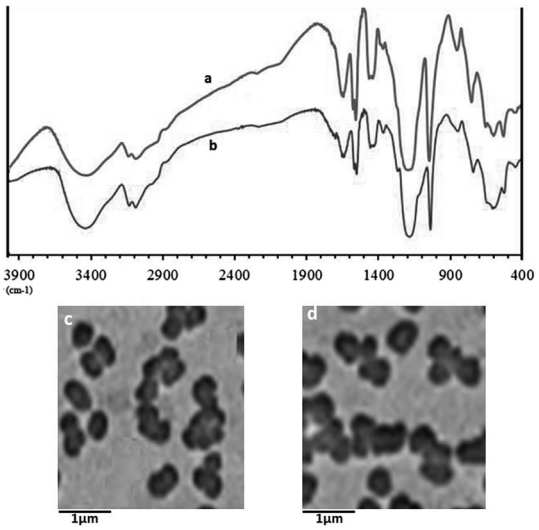


Fig. 7 FT-IR spectra and the Transmission electron microscope (TEM) images of the fresh catalyst (a and c), and the used catalyst after 6 cycles (b and d).

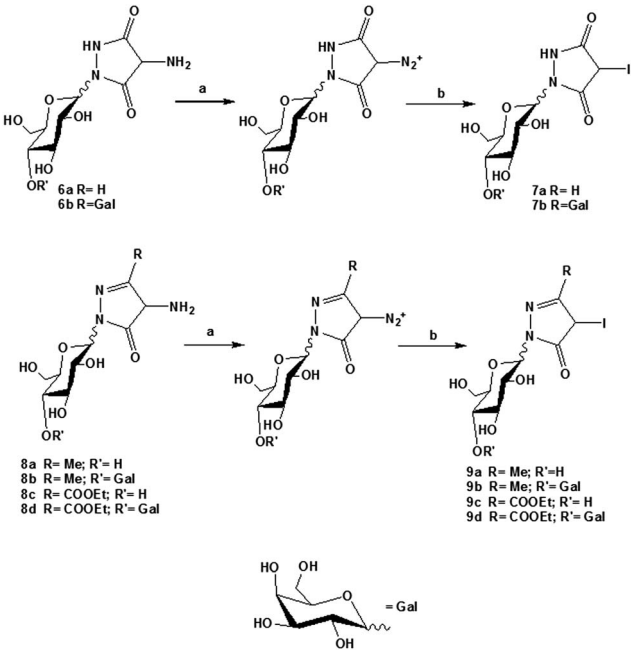


Scheme 3 Synthesis of the pyrazolidine-3,5-dione iodides **7a,b**, and pyrazolin-5-one iodides **9a–d** by using $Fe_3O_4$@SILnP as catalyst. Reagents and conditions (a) $NaNO_2$, $Fe_3O_4$@SILnP, drops of $H_2O$, 0 °C (b) NaI, 0 °C to RT.

led to lower yields of the expected iodoarenes whilst the yields of phenol by-products were higher. It should be noted that this reaction procedure requires the addition of a small amount of water to generate the wet $Fe_3O_4$@SILnP sulfuric acid, and must be carried out in a stepwise manner in order to obtain good yields.

At the end of iodination reaction and the products had been isolated, the catalyst was magnetically separated and washed several times with water and methanol to ensure unreacted reactive does not remain on the surface of magnetic nanoparticles. It should be noted that the aryldiazonium salts supported on $Fe_3O_4$@SILnP were stable to be kept at room temperature and could be stored for 48 h in a desiccator without any loss of activity.

The investigation of a solvent-free diazotization–iodination reaction using $Fe_3O_4$@SILnP was repeated six times to evaluate the catalyst recyclability and stability (Fig. 6). After each run, the catalyst was separated from the reaction mixture by an applied magnetic field, washed with water and methanol and reused in the next cycle, which indicates the high stability of the catalyst under these reaction conditions.

The recovered catalyst after six runs had no obvious change in structure, referring to the FT-IR spectra in comparison with the fresh one (Fig. 7a and b). A TEM observation of the recovered catalyst was also made, and there were no obvious changes in morphology and size (Fig. 7c and d). These results revealed that the catalyst was very stable and could endure these reaction conditions.

Table 2 reports the efficiency comparison between our method for the diazotization–iodination of aromatic amines and others some others published works in literature. Each of

Table 2 Comparison of results using $Fe_3O_4$@SILnP/$NaNO_2$/NaI with results obtained by other works for the diazotization–iodination of 4-nitro aniline

| Entry | Reagents | Conditions | Time (min) | Yield | Ref. |
|---|---|---|---|---|---|
| 1 | HI/$KNO_2$ | DMSO/35 °C | 15 | 89 | 57 |
| 2 | KI/$NaNO_2$/PTSA | MeCN/10–25 °C | 50 | 81 | 58 |
| 3 | $NaNO_2$/sulfonated-resin/KI | $H_2O$/RT | 90 | 71 | 59 |
| 4 | PTSA/$NaNO_2$/KI | Water-paste form | 20–30 | 72 | 60 |
| 5 | Wet SSA/$NaNO_2$/KI | Solvent free/RT | 30 | 83 | 61 |
| 6 | Resin $NO_2^-$, *p*-TsOH, $H_2O$ | KI/RT | 90 | 91 | 56 |
| 7 | [H-NMP]$HSO_4$, $NaNO_2$, NaI | Solvent-free/RT | 20–30 | 85 | 62 |
| 8 | [P4-VP][a]$NO_2$/$H_2SO_4$/KI | Water/0–60 °C | 100 | 74 | 63 |
| 9 | $Fe_3O_4$@SILnP/$NaNO_2$/NaI | Solvent-free/RT | 14 | 82 | This work |
| 10 | [H-NMP]$HSO_4$@$SiO_2$ | Water/RT | 14 | 59 | This work |

[a] Poly(4-vinylpyridine).

Published on 15 September 2014. Downloaded by Nipissing University on 17/10/2014 17:30:54.

Table 3 Synthesis of **7a**, **9a** and **9c** in the presence of various amount of $Fe_3O_4$@SILnP as catalyse at 0 °C to room temperature

| Entry | Substrate | Time (min) | Catalyst (mg) | Yield % |
|---|---|---|---|---|
| 1 | **7a** | 25 | 100 | 51 |
| 2 | **7a** | 20 | 150 | 74 |
| 3 | **7a** | 12 | 200 | 89 |
| 4 | **7a** | 12 | 300 | 89 |
| 5 | **9a** | 25 | 100 | 49 |
| 6 | **9a** | 20 | 150 | 77 |
| 7 | **9a** | 1 | 200 | 87 |
| 8 | **9a** | 14 | 300 | 87 |
| 9 | **9c** | 25 | 100 | 54 |
| 10 | **9c** | 20 | 150 | 69 |
| 11 | **9c** | 14 | 200 | 89 |
| 12 | **9c** | 14 | 300 | 89 |

these methods have their own advantages, but they often some limitations such as the use of organic solvent, necessity of temperature control (entries 1, 2 and 8), long reaction time (entries 2, 3, 5 and 6) and employ of non-recyclable catalyst (entry 4). The use of $Fe_3O_4$@SILnP as a catalyst in the diazotization–iodination of the different aromatic amines afford the corresponding iodide derivatives in high yield (about 80%) in a shorter reaction time (Table 1). This was presumed to occur due to the adsorption of reactants on the surface of the nano-support, increasing the local concentration of reactants around the active sites of the $Fe_3O_4$@SILnP and promotes the reaction effectively. In addition, this novel catalyst showed a higher yield in comparison with [H-NMP]$HSO_4$@$SiO_2$ (Table 2, entry 10), which indicated that the smaller particle mitigated more diffusion effects and then accelerated the reaction.

When using a supported catalyst, there is a possibility that the active species might migrate from the solid support to the liquid phase, since the leached active ones become responsible for the good catalytic activity. In order to extend the use of our new catalyst based on $Fe_3O_4$@SILnP in the diazotization–iodination, other aromatic amines based on the pyrazolidine-3,5-dione **6a,b**, and pyrazolin-5-one **8a–d** were used to synthesis their corresponding halide derivatives **7a,b** and **9a–d** respectively, by the treatment of the formed diazonium salts with NaI as reported in the Scheme 3.

Initially, to optimize the reaction conditions, the reaction of **6a**, **8a** and **8c** (1 mmol) were studied as a simple model using different quantities of catalyst (Table 3). It was found that the best result was obtained when the reaction was carried out in the presence of 200 mg of catalyst (Table 3, Entry 3, 7, 11).

The different pyrazolidine-3,5-dione amines **6a,b**, and pyrazolin-5-one amines **8a–d** were transformed rapidly into the corresponding iodides derivatives in good yields under solvent-free conditions as reported in Table 4. However, the corresponding phenol by-products were formed only in trace yields. Also, the effect of the solvent on this reaction was also studied by using the water as solvent, under the same conditions, and the results show lower yields of the expected iodoarenes whilst the yields of phenol by-products were higher, which confirm the results obtained with the aniline derivatives **4a–f**.

Table 4 Iodination of pyrazolidine-3,5-dione amines **6a,b**, and pyrazolin-5-one amines **8a–d** with $Fe_3O_4$@SILnP/$NaNO_2$/NaI/at 0 °C to room temperature

| Entry | Substrate | Time (min) diazotization–iodination | Yield |
|---|---|---|---|
| 1 | **7a** | 6/6 | 89 |
| 2 | **7b** | 6/6 | 88 |
| 3 | **9a** | 8/6 | 87 |
| 4 | **9b** | 8/6 | 89 |
| 5 | **9c** | 8/6 | 89 |
| 6 | **9d** | 8/6 | 88 |

# Experimental methods and characterization

### Materials

All chemicals were reagent grade (Aldrich Chemical Co.) and were used as purchased without further purification. Thin layer chromatography (TLC) analysis was performed using Fluka aluminium foils coated with 25 mm particle size silica gel matrix F254. TLC development involved either UV (254 and 366 nm) or visible light inspection, followed by either treatment with an acid solution of *p*-anisaldehyde or a basic solution of $KMnO_4$ and heating. Flash column chromatography was performed on Merck silica gel 60 (particle size 0.040–0.063 nm, 230–400 mesh ASTM) UV-vis spectra were recorded on a Cary-4000 Varian spectrophotometer, using either 0.1 or 1 cm quartz cuvettes. Infra-red spectra were recorded in KBr disk on a Perkin Elmer-Spectrum BX FTIR system. Absorptions are quoted in wavenumbers ($cm^{-1}$). $^1H$ and $^{13}C$ NMR spectra were recorded at 200 MHz $^1H$ (50.0 MHz $^{13}C$) on a Varian Gemini spectrometer. Spin resonances are reported as chemical shifts ($\delta$) in parts per million (ppm) and referenced to the residual peak as an internal standard of the solvent employed, as follow: $CDCl_3$ 7.27 ppm ($^1H$ NMR), 77 ppm ($^{13}C$ NMR, central band), $DMSOd_6$ 2.50 ppm ($^1H$ NMR, central band), 39.5 ppm ($^{13}C$ NMR, central band). Spin multiplicity is showed by s = singlet, d = doublet, t = triplet, q = quartet, m = multiplet, br = broad. Coupling constants *J* are reported in Hertz. Mass spectra were recorded on a ThermoScientific LCQ-Fleet mass spectrometer under electrospray ionization (ESI, +c or −c technique). High Resolution Mass Spectra (HRMS) were recorded on an LTP Orbitrap mass spectrometer from Thermo Electron Corporation under ESI (+c) technique. Mass spectrometric analysis is quoted in the *m*/*z* form. Elemental analyses were recorded on a Perkin Elmer 240C Elemental Analyzer. Thermogravimetric analysis (TGA) of the samples was performed using a Perkin Elmer Diamond Thermogravimeter. Dried samples was placed in the TGA furnace and heated at a rate of 10 °C/inform room temperature to 700 °C in static air. The fluorescence spectra were measured by Hitachi F-4500 fluorescence spectrophotometer with a 1 cm quartz cell. Doubly distilled deionized water (DIW) was used for all experiments. In this study, only distilled water was used. The pyrazolidine-3,5-dione **6a,b**, and pyrazolin-5-one **8a–d** were prepared following our previous paper.[64]

 This journal is © The Royal Society of Chemistry 2014

Published on 15 September 2014. Downloaded by Nipissing University on 17/10/2014 17:30:54.

### Colloidal iron oxide nanoparticle synthesis

The magnetite nanoparticles were prepared by the conventional co-precipitation method with some modifications.[65] $FeCl_3 \cdot 6H_2O$ (2.32 g) and $FeCl_2 \cdot 4H_2O$ (0.86 g) were dissolved in 20 mL of the deionized water under nitrogen gas with vigorous stirring at 85 °C. Then, ammoniac solution 25% (3 mL) was added to the solution. The color of bulk solution turned from orange to black immediately. The magnetite precipitates were washed twice with deionized water and once with sodium chloride (0.02 M). The final magnetite nanoparticles were precipitated by magnetic decantation.

Followed Stober method[65] with some modification, coating magnetite nanoparticles with silica was carried out in basic alcohol–water mixture at room temperature by using magnetic fluids as seeds. First, magnetic fluid was diluted with water, alcohol and ammonia aqueous. Then this dispersion was homogenized by ultrasonic vibration in water bath. Finally, under continuous mechanical stirring, TEOS was slowly added to this dispersion, and after stirring for 12 h, silica was formed on the surface of magnetite nanoparticles through hydrolysis and condensation of TEOS.

### Preparation of the acidic ionic liquid 3b

To a solution of pyrrolidin-2-one **1** (1.00 g, 11.76 mmol) in 15 mL dry toluene, (3-chloropropyl)triethoxysilane **2** (2.82 g, 11.76 mmol) was added and the resulting mixture was refluxed for 24 h. After, the solvent was removed under the reduce pressure and the crude product was washed with ether 3 times and dried in vacuum. The formed solid **3a** (95% yield) was dissolved in 10 mL of DCM in a 50 mL round-bottom flask, and equimolar sulfuric acid was slowly added dropwise into the flask at 0 °C. After the dropwise addition was finished, the mixture was heated up to 60 °C gradually and then stirred for 12 h. Finally, the formed liquid was washed with ether 3 times and dried in vacuum at 50 °C for 5 h. $^1$H NMR (200 MHz, $D_2O$): $\delta$ = 3.9 (6H, m, $CH_2$), 3.34–3.22 (4H, m), 2.41–2.30 (4H, m), 1.83 (9H, m, $CH_3$). 0.62 (2H, t, $J$ = 6.4 Hz, $SiCH_2$) ppm. $^{13}$C NMR (50 MHz, $D_2O$): $\delta$ = 188.4, 52.5, 50.2, 41.1, 35.8, 18.4, 17.3, 11.6, 10.4 ppm.

### Surface functionalization of silica coated $Fe_3O_4$ (M/SiNPs) with the ionic liquid 3b

In a round bottom flask, 400 mg of M/SiNPs were suspended in a solution of 30.0 mL of anhydrous toluene, and sonicated for 30 min at rt. The silane **3b** (0.47 g; 0.68 mmol) was hydrolyzed in 25.0 mL of anhydrous toluene and 0.12 mL DIW for 15 min at rt then added to SiNPs suspension and sonicated again for 30 min. The reaction mixture was refluxed for 24 h without magnetic stirring. The magnetic silica nanoparticles modified with ionic liquids SILnP were separated and washed twice with 90% toluene/DIW and 80% EtOH/DIW using centrifugation (11 200*g* for 10 min) technique. Finally, the functionalized SILnP were dried under vacuum at 110 °C for 24 h before use.

### General procedure for preparation of aryl iodides

To a solution of the aromatic amine (1 mmol) and $Fe_3O_4$@SILnP (200 mg) in a few drops of water, $NaNO_2$ (2.5 mmol), was added at 0 °C and the resulting mixture was stirred at room temperature for few minutes. Then, NaI (2.5 mmol) was added to the formed diazonium salt, the iodination reaction began immediately after NaI addition, and the reaction mixture volume increased due to the evolution of nitrogen gas. This one-pot diazotization–iodination process takes about few minutes to complete. After, the reaction; the catalyst was magnetically separated and washed several times with water and methanol to ensure unreacted reactive does not remain on the surface of magnetic nanoparticles. The crude products were purified by recrystallization from ethanol. The recovered catalyst was dried and reused for subsequent runs.

### 4-Iodo-1-(3,4,5-trihydroxy-6-hydroxymethyl-tetrahydro-pyran-2-yl)-pyrazolidine-3,5-dione (7a)

The product **7a** was prepared according to the general procedure in 89% as yield. **7a** is obtained as a colored solid as a mixture of α and β pyranosic anomers. $^1$H NMR (200 MHz, $Me_2SO$): $\delta$ = 5.52 (s, 1H), 5.28–5.22 (d, 1H), 3.82–3.61 (m, 4H), 3.47–3.31 (m, 2H) ppm. $^{13}$C NMR (50 MHz, $Me_2SO$): see Table 5 in the ESI† for the glycidic part and $\delta$ = 170.3, 168.2, 54.5 ppm. MS (ESI): $m/z$ = 389.13 $[M + 1]^+$. $C_9H_{13}IN_2O_7$ (387.98): calcd C, 27.85; H, 3.38; N, 7.22 found: C, 27.97; H, 3.51; N, 7.38.

### 1-[3,4-Dihydroxy-6-hydroxymethyl-5-(3,4,5-trihydroxy-6-hydroxymethyl-tetrahydro-pyran-2-yloxy)-tetrahydro-pyran-2-yl]-4-iodo-pyrazolidine-3,5-dione (7b)

The product **7b** was prepared according to the general procedure in 88% as yield. **7b** is obtained as a colored solid as a mixture of α and β pyranosic anomers. $^1$H NMR (200 MHz, $Me_2SO$): $\delta$ = 5.54 (s, 1H), 5.11–4.55 (m, 2H, both anomers), 4.30–4.15 (m, 4H, both anomers), 3.88–3.79 (m, 6H, both anomers), 3.45–3.42 (m, 2H, both anomers) ppm. $^{13}$C NMR (50 MHz, $Me_2SO$): see Table 6 in the ESI† for the glycidic part and $\delta$ = 170.5, 168.6, 54.8 ppm. MS (ESI): $m/z$ = 551.21 $[M + 1]^+$. $C_{15}H_{23}IN_2O_{12}$ (550.04): calcd C, 32.74; H, 4.21; N, 5.09 found: C, 32.92; H, 4.43; N, 5.23.

### 2-(5-Hydroxy-4-iodo-3-methyl-pyrazole-1-yl)-6-hydroxymethyl-tetrahydro-pyran-3,4,5-triol (9a)

The product **9a** was prepared according to the general procedure in 87% as yield. **9a** is obtained as a colored solid as a mixture of α and β pyranosic anomers. $^1$H NMR (200 MHz, $Me_2SO$): $\delta$ = 11.54 (s, 1H, OH), 5.29–5.21 (d, 1H), 3.81–3.61 (m, 4H), 3.47–3.30 (m, 2H), 2.71 (s, 3H, $CH_3$, Pyr) ppm. $^{13}$C NMR (50 MHz, $Me_2SO$): see Table 5 in the ESI† for the glycidic part and $\delta$ = 155.3, 138.9, 60.5, 12.8 ppm. MS (ESI): $m/z$ = 387.23 $[M + 1]^+$. $C_{10}H_{15}IN_2O_6$ (386.00): calcd C, 31.10; H, 3.92; N, 7.25 found: C, 31.23; H, 4.11; N, 7.39.

Published on 15 September 2014. Downloaded by Nipissing University on 17/10/2014 17:30:54.

**2-[4,5-Dihydroxy-6-(5-hydroxy-4-iodo-3-methyl-pyrazol-1-yl)-2-hydroxymethyl-tetrahydro-pyran-3-yloxy]-6-hydroxymethyl-tetrahydro-pyran-3,4,5-triol (9b)**

The product **9b** was prepared according to the general procedure in 88% as yield. **9b** is obtained as a colored solid as a mixture of α and β pyranosic anomers. $^1$H NMR (200 MHz, $Me_2SO$): $\delta = 11.58$ (s, 1H, OH), 5.11–4.57 (m, 2H, both anomers), 4.31–4.13 (m, 4H, both anomers), 3.88–3.78 (m, 6H, both anomers), 3.44–3.41 (m, 2H, both anomers), 2.73 (s, 3H, $CH_3$, Pyr) ppm. $^{13}$C NMR (50 MHz, $Me_2SO$): see Table 6 in the ESI† for the glycidic part and $\delta = 155.7$, 138.3, 60.2, 12.6 ppm. MS (ESI): $m/z = 549.28$ $[M + 1]^+$. $C_{16}H_{25}IN_2O_{11}$ (548.05): calcd, 35.05; H, 4.60; N, 5.11 found: 35.23; H, 4.77; N, 5.24.

**5-Hydroxy-4-iodo-1-(3,4,5-trihydroxy-6-hydroxymethyl-tetrahydro-pyran-2-yl)-1*H*-pyrazole-3-carboxylic acid ethyl ester (9c)**

The product **9c** was prepared according to the general procedure in 89% as yield. **9c** is obtained as a colored solid as a mixture of α and β pyranosic anomers. $^1$H NMR (200 MHz, $Me_2SO$): $\delta = 11.55$ (s, 1H, OH), 5.28–5.21 (d, 1H), 4.25 (q, 2H, $CH_2$), 3.82–3.60 (m, 4H), 3.48–3.31 (m, 2H), 1.33 (t, 3H, $CH_3$) ppm. $^{13}$C NMR (50 MHz, $Me_2SO$): see Table 5 in the ESI† for the glycidic part and $\delta = 159.6$, 151.2, 62.1, 58.3, 13.7 ppm. MS (ESI): $m/z = 445.23$ $[M + 1]^+$. $C_{12}H_{17}IN_2O_8$ (444.03): calcd C, 27.85; H, 3.38; N, 7.22; C, 32.45; H, 3.86; N, 6.31 found: C, 32.57; H, 3.98; N, 6.45.

**1-[3,4-Dihydroxy-6-hydroxymethyl-5-(3,4,5-trihydroxy-6-hydroxymethyl-tetrahydro-pyran-2-yloxy)-tetrahydro-pyran-2-yl]-5-hydroxy-4-iodo-1*H*-pyrazole-3-carboxylic acid ethyl ester (9d)**

The product **9d** was prepared according to the general procedure in 88% as yield. **9d** is obtained as a colored solid as a mixture of α and β pyranosic anomers. $^1$H NMR (200 MHz, $Me_2SO$): $\delta = 11.56$ (s, 1H, OH), 5.12–4.56 (m, 2H, both anomers), 4.31–4.12 (m, 6H, both anomers), 3.88–3.78 (m, 6H, both anomers), 3.46–3.41 (m, 2H, both anomers), 1.32 (t, 3H, $CH_3$) ppm. $^{13}$C NMR (50 MHz, $Me_2SO$): see Table 6 in the ESI† for the glycidic part and $\delta = 155.7$, 138.3, 60.2, 12.9 ppm. MS (ESI): $m/z = 549.28$ $[M + 1]^+$. $C_{16}H_{25}IN_2O_{11}$ (548.05): calcd, 35.05; H, 4.60; N, 5.11 found: 35.23; H, 4.77; N, 5.24.

## Conclusions

In summary, we have developed an efficient and experimentally simple method for the diazotization–iodination of aromatic amines in the presence of *N*-propyl-2-pyrrolidonium hydrogen sulfate ([H-NPP]$HSO_4$) supported on nano-sized silica-coated magnetite as acid catalyst under solvent-free conditions in good to excellent yields. The sequential diazotization–iodination take place in the presence of the acidic $Fe_3O_4$@SILnP as a mild and new proton source and the resulting diazonium salts are stable and react rapidly with potassium iodide to produce aryl iodides.

## Acknowledgements

This work is financially supported by GEMTEX Laboratory France. We thank Mr Christian Catel (technician of GEMTEX laboratory) for its kind disponibility.

## Notes and references

1 K. Hunger, *Industrial Dyes: Chemistry, Properties, Applications*, Wiley-VCH, Weinheim, Germany, 2003.
2 A. Bafana, S. S. Devi and T. Chakrabarti, *Environ. Rev.*, 2011, **19**, 350.
3 R. Bianchini, G. Catelani, E. Frino, J. Isaad and M. Rolla, *BioResources*, 2007, **2**, 630.
4 R. Bianchini, G. Catelani, R. Cecconi, F. D'Andrea, L. Guazzelli, J. Isaad and M. Rolla, *Eur. J. Org. Chem.*, 2008, **3**, 444.
5 R. Bianchini, G. Catelani, R. Cecconi, F. D'Andrea, E. Frino, J. Isaad and M. Rolla, *Carbohydr. Res.*, 2008, **343**, 2067.
6 J. Isaad, M. Rolla and R. Bianchini, *Eur. J. Org. Chem.*, 2009, 2748.
7 J. Isaad, F. Malek and A. El Achari, *Dyes Pigm.*, 2012, **92**, 1212.
8 R. Bianchini, M. Rolla, J. Isaad, G. Catelani, L. Guazzelli, M. Corsi and M. Bonanni, *Carbohydr. Res.*, 2012, **356**, 104.
9 J. Isaad and A. Perwuelz, *Tetrahedron Lett.*, 2010, **51**, 5328.
10 V. Pasquet, N. Behary, A. Perwuelz and J. Isaad, *Fibers Polym.*, 2013, **14**, 1141.
11 J. Isaad, *Tetrahedron*, 2013, **69**, 2239.
12 J. Isaad and F. salaun, *Sens. Actuators, B*, 2011, **157**, 26.
13 J. Isaad and A. El achari, *Anal. Chim. Acta*, 2011, **694**, 120.
14 J. Isaad and A. El Achari, *Tetrahedron*, 2011, **67**, 4196.
15 J. Isaad and A. El Achari, *Tetrahedron*, 2011, **67**, 4939.
16 J. Isaad and A. El achari, *Tetrahedron*, 2011, **67**, 5678.
17 J. Isaad and A. Perwuelz, *Tetrahedron Lett.*, 2010, **51**, 5810.
18 J. Dakin and B. Culshaw, *Optical Fiber Sensors*, Artech House, Boston-London, 1997, vol. IV, ch. 8, pp. 53–107.
19 Z. Czech, A. Butwin, E. Herko, B. Hefczyc and J. Zawadiak, *eXPRESS Polym. Lett.*, 2008, **12**, 277.
20 X. Tong, G. Wang and Y. Zhao, *J. Am. Chem. Soc.*, 2006, **128**, 8746.
21 H. Durr and H. Bouas-Laurent, *Photochromism: Molecules and Systems*, Elsevier, Amsterdam, 2003.
22 A. Zarei, A. R. Hajipour, L. Khazdooz, B. F. Mirjalili and R. A. Najafi, *Dyes Pigm.*, 2009, **81**, 240.
23 A. Morsy and M. El-Apasery, *J. Appl. Polym. Sci.*, 2008, **109**, 695.
24 N. Noroozi-Pesyan, J. Khalafy and Z. Malekpoor, *Progress in Color Colorants and Coatings*, 2009, **1**, 61.
25 N. Noroozi-Pesyan, J. Khalafy and Z. Malekpoor, *J. Chin. Chem. Soc.*, 2009, **56**, 1018.
26 Y. Moglie, C. Vitale and G. Radivoy, *Tetrahedron Lett.*, 2008, **49**, 1828–1831.
27 F. Ahmed Khan, J. Dash, C. Sudheer and R. K. Gupta, *Tetrahedron Lett.*, 2003, **44**, 7783.
28 B. J. P. Whalley, H. G. V. Evans and C. A. Winkler, *Can. J. Chem.*, 1956, **34**, 1154.

 This journal is © The Royal Society of Chemistry 2014

Published on 15 September 2014. Downloaded by Nipissing University on 17/10/2014 17:30:54.

29 D. A. Blackadder and C. Hinshelwood, *J. Chem. Soc.*, 1957, 2904.
30 J. A. Hyatt, *Tetrahedron Lett.*, 1977, **18**, 141.
31 T. Mukaiyama, H. Nambu and M. Okamoto, *J. Org. Chem.*, 1962, **27**, 3651.
32 G. A. Olah, B. G. Balaram Gupta and S. C. Narang, *J. Org. Chem.*, 1978, **43**, 4503.
33 R. Sanz, J. Escribano, Y. Fernandez, R. Aguado, M. R. Pedrosa and F. J. Arnaiz, *Synlett*, 2005, 1389.
34 T. F. Chung, Y. M. Wu and C. H. Cheng, *J. Org. Chem.*, 1984, **49**, 1215.
35 K. Ohe, S. Uemura, N. Sugita, H. Masuda and T. Taga, *J. Org. Chem.*, 1989, **54**, 4169.
36 S. Wada, M. Urano and H. Suzuki, *J. Org. Chem.*, 2002, **67**, 8254.
37 A. Lycka, A. Kolonicny, P. Simunek and V. Machacek, *Dyes Pigm.*, 2007, **72**, 208.
38 H. Valizadeh and A. Shomali, *Dyes Pigm.*, 2012, **92**, 1138.
39 D. L. Astolfi and F. C. Mayville, *Tetrahedron Lett.*, 2003, **44**, 9223.
40 A. R. Hajipour, A. Rajaei and A. E. Ruoho, *Tetrahedron Lett.*, 2009, **50**, 708.
41 A. R. Hajipour, L. Khazdooz and A. E. Ruoho, *Catal. Commun.*, 2008, **9**, 89.
42 M. J. Earle and K. R. Seddon, *Pure Appl. Chem.*, 2000, **72**, 1391.
43 A. C. Cole, J. L. Jensen, I. Ntai, K. L. T. Tran, K. J. Weaver, D. C. Forbes and J. H. Davis, *J. Am. Chem. Soc.*, 2002, **124**(21), 5962.
44 N. Yan, Y. Yuan, R. Dykeman, Y. Kou and P. J. Dyson, *Angew. Chem., Int. Ed.*, 2010, **49**, 5549.
45 A. Riisager, R. Fehrmann and M. Haumann, *Top. Catal.*, 2006, **40**, 91.
46 C. P. Mehnert, *Chem.–Eur. J.*, 2005, **11**, 50.
47 C. P. Mehnert, R. A. Cook, N. C. Dispenzire and M. Afeworki, *J. Am. Chem. Soc.*, 2002, **124**, 12932.
48 M. H. Valkenberg, C. de Castro and W. F. H. Olderich, *Top. Catal.*, 2001, **14**, 139.
49 A. Wolfson, I. F. J. Vankelecom and P. A. Jacobs, *Tetrahedron Lett.*, 2003, **44**, 1195.
50 J. Huang, T. Jiang, H. Gao, B. Han, Z. Liu, W. Wu, Y. Chang and G. Zhao, *Angew. Chem., Int. Ed.*, 2004, **43**, 1397.
51 B. Kalpesh, A. Sidhpuria, L. Daniel-da-Silva, T. Trindade and J. A. P. Coutinho, *Green Chem.*, 2011, **13**, 340.
52 J. Isaad and A. El Achari, *Dyes Pigm.*, 2013, **99**, 878.
53 J. Isaad and A. El Achari, *Tetrahedron*, 2013, **69**, 4866.
54 A. Hu, G. T. Yee and W. Lin, *J. Am. Chem. Soc.*, 2005, **127**, 12486.
55 Q. Chang, L. H. Zhu, C. Yu and H. Q. Tang, *J. Lumin.*, 2008, **128**, 1890.
56 A. Zarei, A. R. Hajipour and L. Khazdoozd, *Synthesis*, 2009, **6**, 941–944.
57 W. Baik, W. Luan, H. J. Lee, C. H. Yoon, S. Koo and B. H. Kim, *Can. J. Chem.*, 2005, **83**, 213–219.
58 E. A. Krasnokutskaya, N. I. Semenischeva, V. D. Filimonov and P. Knochel, *Synthesis*, 2007, **1**, 81–84.
59 V. D. Filimonov, N. I. Semenischeva, E. A. Krasnokutskaya, A. N. Tretyakov, H. Y. Hwang and K. W. Chi, *Synthesis*, 2008, **2**, 185–187.
60 D. A. Gorlushko, V. D. Filimonov, E. A. Krasnokutskaya, N. I. Semenischeva, B. S. Go, H. Y. Hwang, E. H. Cha and K.-W. Chi, *Tetrahedron Lett.*, 2008, **49**, 1080–1082.
61 H. Zollinger, in *Diazo Chemistry I, Aromatic and Heteroaromatic Compounds*, VCH, 1994, p. 25.
62 A. Hajipour and F. Mohammadsaleh, *Iran. J. Chem. Chem. Eng.*, 2011, **30**, 23–28.
63 M. A. Karimi Zarchi and N. Ebrahimi, *J. Appl. Polym. Sci.*, 2011, **121**, 2621–2625.
64 J. Isaad, *Tetrahedron*, 2013, **69**, 2239–2250.
65 W. Stober, A. Fink and E. Bohn, *J. Colloid Interface Sci.*, 1968, **26**, 62.